

---

| RESEARCH ARTICLE

## Assessment of Fluvial Dynamics of Bakiya River, Central Nepal Using Stream Classification

Kishor Rimal<sup>1</sup>, Naresh Kazi Tamrakar<sup>2</sup> ✉ Sujan Bista<sup>3</sup>, Dinesh Raj Sharma<sup>4</sup> and Arju Bhattarai<sup>5</sup>

<sup>1234</sup>Central Department of Geology, Tribhuvan University, Kirtipur, Kathmandu, Nepal

**Corresponding Author:** Naresh Kazi Tamrakar, **E-mail:** [naresh.tamrakar@cdgl.tu.edu.np](mailto:naresh.tamrakar@cdgl.tu.edu.np)

---

### | ABSTRACT

Using the Rosgen Stream Classification System (RSCS), this study investigates the hydrological features and fluvial morphology of the Bakiya River, a seventh-order stream that traverses the Siwalik and Indo-Gangetic plains of Central Nepal. An extensive assessment of morpho-hydraulic parameters and sediment size distribution across 17 transects was made by a combination of field surveys and GIS-based analyses. The majority of the transects were classified as C4 streams, which are distinguished by meandering channels that are gravel-dominated, slightly entrenched, and connected to floodplains. The stream types B4, F4, and E4 have also been identified, which all display unique hydrological and geomorphic characteristics. The study found that human activity sediment deposition and tributary inputs all affected downstream changes in channel morphology. Vegetation played a crucial role in stabilizing streambanks, and areas with higher erosion susceptibility and entrenchment were identified as priority zones for engineered interventions. The research enhances our understanding of river stability and provides useful guidance for sustainable watershed management and restoration by combining Rosgen classification principles with localized geomorphic and anthropogenic features.

### | KEYWORDS

Watershed study, Fluvial morphology, Rosgen stream classification, Sediment transport, Stream management

### | ARTICLE INFORMATION

**ACCEPTED:** 21 December 2024

**PUBLISHED:** 03 February 2025

**DOI:** 10.61424/ijans.v3.i1.188

---

## 1. Introduction

Rosgen Stream Classification System (RSCS) offers a structured framework for classifying rivers based on their morphological characteristics, facilitating communication between researchers and experts from different fields (Rosgen, 1994). RSCS uses various morphological characteristics to classify streams. It focuses on understanding stream dynamics and how they interact with the environment and attempts to examine fluvial geomorphology and hydrology. As this classification provides a systematic framework for assessing stream stability, predicting stream behavior, and assisting with watershed management, it aids in planning for the conservation and restoration of streams and their ecosystems. Rosgen classification is distinct because it employs a hierarchical method and field-based measurements with geomorphic principles to divide streams into various types. Schumm's process-based classification (Schumm, 1977) or the Leopold and Wolmans channel pattern classification (Leopold & Wolman, 1957) focuses more on specific elements such as stream processes or patterns. The Rosgen method provides a comprehensive and visually appealing framework that makes it appropriate for both scientific research and real-world applications.

RSCS is often applied to understand stream morphology for ecological conservation hazard management or infrastructure planning. In order to inform sustainable watershed management strategies, these studies typically

seek to identify stream types for restoration planning, evaluate the effects of land use changes, and forecast potential stream responses to environmental stressors. This study can also help us understand fluvial processes and their importance for maintaining stream health in the face of human and climatic stressors. This tool forecasts river behavior and understands channel dynamics to support management and restoration efforts. While some classification schemes, such as the (Rust, 1977) system, focus on traits like braiding and sinuosity for alluvial channels, other schemes, such as process-based approaches like (Montgomery, 1993) methods, emphasize sediment transport and geomorphic processes. The Rosgen Level II classification system provides detailed morphological descriptions of streams by assessing features such as bed materials and entrenchment channel patterns and profiles (Rosgen, 1994). With only minor adjustments for various slope types, it has been effectively applied in a range of settings (Castro & Jackson, 2001; Jefferson N. Keaton, 2005; Savery et al., 2001).

The Bakiya River is located in Central Nepal (Figure 1). It is a seventh-order stream that drains roughly 317 square kilometers in the Lesser Himalayas, Siwalik region, and Indo Gangetic Plain. In this study, the river is categorized using the RSCS. Bounded by the Bagmati Watershed to the north and east and the Karra Khola Watershed to the west, the Bakiya Rivers hydrological and geomorphological characteristics show that it serves as an important drainage system that with tributaries such as Bandere Khola, Chyauchyu Khola, and Phirke Khola. It has been considered as a future prospective region owing to two national projects around this area that include the extension of countries middle region highways, the Kathmandu-Terai/Madhesh Fast Track, as well as the Nijgadh International Airport. The study uses RSCS Level II morphological classification to provide insight into geomorphic processes' stability and the Bakiya Rivers' restoration potential, which aids in predicting river behavior, understanding sediment transport dynamics, and identifying unstable areas. Classification is essential to sustainable watershed management and helps hydrologists, geomorphologists, and environmental planners to communicate across disciplines. This study aids in the creation of effective plans for erosion control, ecological restoration, and sustainable land use. The study's primary objectives are to classify the Bakiya River, assess stream stability, generate a scientific understanding of river morphology in Nepal's Siwalik region, and provide recommendations for watershed management.

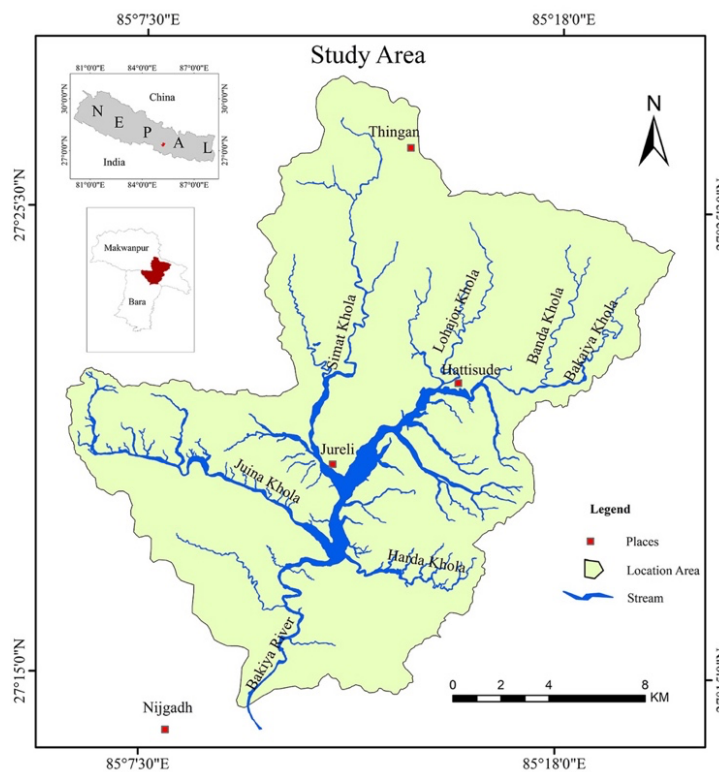


Figure 1: Location map of the study area

## 2. Geological Setting

The Siwalik Range in Nepal, a young and fragile sedimentary formation, is highly susceptible to landslides and debris flows due to its weak geological composition and heavy rainfall (Bhandari & Dhakal, 2018, 2019, 2020). Studies in the Babai watershed reveal that landslides are predominantly controlled by lithology, with the Middle Siwaliks experiencing the highest landslide density (Bhandari & Dhakal, 2018). Debris flows, commonly triggered by landslides on steep slopes, are classified into three types: slide-induced, fall-induced, and erosion-induced, with slide-induced being the most prevalent (Bhandari & Dhakal, 2019, 2020). The average 24-hour rainfall threshold for debris flow occurrence is 160.67 mm (Bhandari & Dhakal, 2019). Landslides in the region exhibit dynamic behavior, showing reactivation, expansion, and occasional self-stabilization over time (Bhandari & Dhakal, 2020). These findings are crucial for understanding landslide mechanics and developing effective management strategies in the Siwalik zone. The Siwalik Range, known as the Sub-Himalaya in Nepal, is a relatively young mountain range. It emerged during the Tertiary Period and has been undergoing deformation for millions of years up to the present (Kizaki, 1994; T et al., 1988; Tokuoka, 1992). The Bakiya watershed lies within the Siwaliks, Indo-Gangetic plains, Mahabharat hills, and Lesser Himalaya (Department of Mines and Geology, 2002) (Figure 2). The Siwaliks are comparatively weaker zones, and the heavy precipitation in the area makes this region more vulnerable to flooding. The increasing population and potential for urbanization make this area a suitable location for research. The river originates in the Lesser Himalaya and includes tributaries such as the Hurnamadi Khola. The topography and drainage characteristics, including prominent valleys and ephemeral streams like Simat Khola, Juina Khola, and Hiramani Khola, contribute to the river's geomorphology. These features are essential for establishing channel planform patterns and applying Rosgen channel classification. The observed drainage pattern, ranging from trellis to dendritic, provides crucial context for applying Rosgen classification principles.

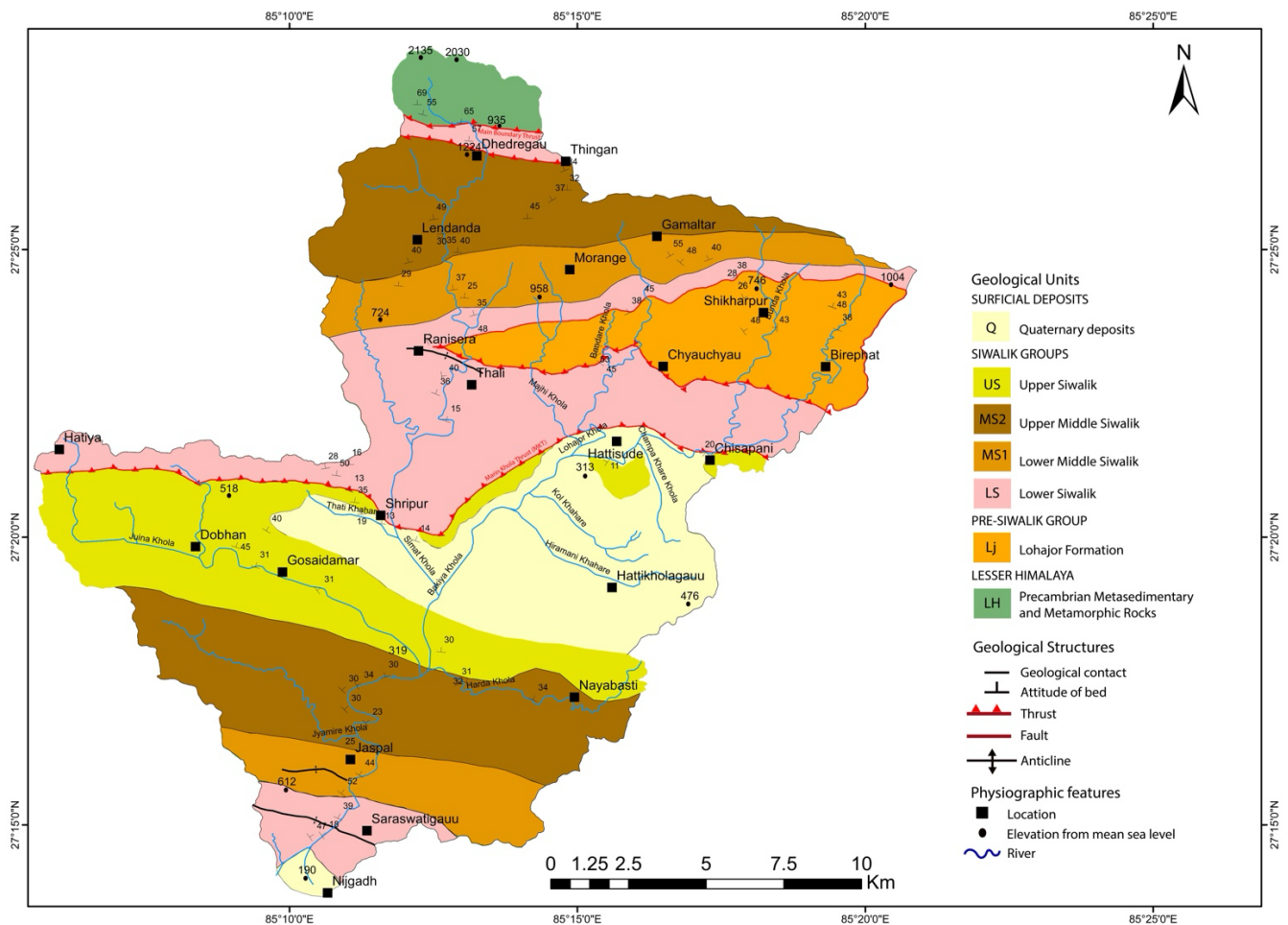


Figure 2: Geological Map of Bakiya watershed (compiled after DMG, 2002)

### 3. Methodology

#### 3.1 Watershed scale parameters

Level I classification comprehensively describes streams based on planform basin relief landform and valley morphology using topographic maps and aerial photography. As confirmed by field reconnaissance, it classifies stream types (A through G) using plan view characteristics- such as straight sinuous or braided channels. Level II classification provides a thorough morphological description by assessing bed materials patterns, dimensions patterns, and channel entrenchment. Understanding sediment supply stream sensitivity and habitat potential requires understanding key parameters such as slope sinuosity entrenchment ratio, width-to-depth ratio, and dominant bed material (Rosgen, 1994).

The study used digital shape files for stream contours and land use from GIID (Geographic Information Infrastructure Division) and 1994 topographic sheets (1:25000 scale) from the Nepalese Survey Department. River cross-sections, sediment size, and channel dimensions were measured in field surveys, and the ESRI's 2020 Global Land Cover Map was used for land use mapping, which was confirmed by field observation. GIS was used for geomorphological analysis, which included thalweg measurements to calculate the sinuosity index, slope, hill shade, drainage patterns, and watershed delineation.

#### 3.2 Cross-section Survey

The cross-section survey is crucial to the Rosgen channel classification system, requiring instruments such as measuring tapes, staff, and level meters. To study the characteristics of the Bakiya River, 17 transects were selected and spaced at equal intervals (Figure 4). Cross-section outlines were created by taking depth measurements across the river channel, recording sediment size distribution (50 samples per cross-section for Wolman pebble counting), and noting key morphohydraulic parameters such as bankfull height at the right and left edges (REW and LEW) and thalweg depth (Figure 5). Measurements of **bankfull width, depth, and cross-sectional area** provided the foundation for assessing channel geometry, while **width-to-depth ratio, entrenchment ratio, and channel slope** were calculated to classify streams into types A to G. Thalweg depths were recorded 100 meters upstream and downstream (200 meters total) to determine water slope, bed slope, and sinuosity, critical for understanding flow dynamics and energy gradients. The **grain size distribution** data, derived from substrate composition, provided insights into sediment transport. This methodological framework ensures accurate classification and supports detailed hydrological and geomorphological analyses for stream management.

#### 3.3 Longitudinal Survey

Thalweg depths were measured along a 200-meter stretch, 100 meters upstream and downstream from each cross-section, in order to evaluate the stream surface slope and stream bed slope as part of the Rosgen stream classification. The stream surface slope was calculated by measuring the elevation of the water surface at regular intervals with a staff and level meter and calculating the variations in elevation between points. Similarly, the elevations of the channel bottom were measured at appropriate intervals to determine the bed slope. These measurements gave vital information for assessing the stream's energy gradient, which affects sediment transport and flow properties. Understanding the hydraulic behavior of streams and dividing them into Rosgen types depends on the accurate determination of these slopes.

#### 3.4 River discharge, velocity, and competency of River

Sediment size data of 17 transects were plotted on a logarithmic graph (sediment size vs. median bed material to calculate Mannings 'n' base values and cumulative frequency) to compute d50 and d84 (Arcement & Schneider, 1989). The slope was measured using leveling tools and survey staff, and n-values (n1, n2, n3, n4) were calculated after adjusting for channel roughness factors (Aldridge & Garrett, 1973) and degree of meandering based on field observations.

(Cowan, 1956) gave the formula for calculating Manning's roughness coefficient "n" value for a channel as:

$$n = (n_b + n_1 + n_2 + n_3 + n_4) m \dots \dots \dots \text{equation (i)}$$

where,

Manning's  $n$  is a roughness coefficient influenced by several factors: the base value ( $n_b$ ), degree of irregularity ( $n_1$ ), variation in channel cross-section ( $n_2$ ), effect of obstructions ( $n_3$ ), amount of vegetation ( $n_4$ ), and degree of meandering and sinuosity ( $m$ ). Manning (1889) gave the formula to calculate the discharge ( $Q$ ) given by:

$$Q = (1.486/n) * A * R^{2/3} * S^{1/2} \dots\dots\dots \text{equation (ii)}$$

$$V = Q/A \dots\dots\dots \text{equation (iii)}$$

(Chow, 1959) gave the formula to calculate boundary shear stress as;

$$\tau_b = \gamma \cdot R \cdot S \dots\dots\dots \text{equation (iii)}$$

(Shields, 1936) defined entrainment function, when the flow exerts shear stress ( $\tau_c$ ) on the bed consisted of sediment particles with diameter  $D$ ;

$$\tau_c = \theta_c (\rho_s - \rho) \cdot g \cdot D_{50} \dots\dots\dots \text{equation (iv)}$$

$$\Omega = \gamma \cdot Q \cdot S \dots\dots\dots \text{equation (v)}$$

where,

$Q$  is the discharge in cubic meters per second,  $V$  is the velocity in meters per second,  $\tau_b$  is the boundary shear stress in newton per meter square,  $\tau_c$  is the critical shear stress in newton per meter square,  $\theta_c$  is the shield parameter,  $\rho_s$  is the density of sediment,  $\rho$  is the density of water,  $g$  is the acceleration due to gravity,  $D_{50}$  is the median grain size,  $\Omega$  is the stream power in newton per slope per meter,  $\gamma$  is the specific weight of water,  $n$  is the Manning's roughness coefficient,  $A$  is the cross-sectional area of the flow in square meters,  $R$  is the hydraulic radius in meters, and  $S$  is the dimensionless channel slope.

## 4. Results

### 4.1 Geomorphological setting of the Bakiya watershed

The Bakiya River is the primary drainage source for the Bakiya watershed, which is situated in Central Nepal, having a perimeter of 104 km and an area of 317 square kilometers. In the middle of the Siwalik region the Bakiya River flows from northeast to southwest. The watershed is bounded to the north and east by the Bagmati Watershed and to the west by the Karra Khola watershed. Bandere Khola Chyauchyau Khola and Phirke Khola are the principal tributaries. The river system plays very important role in sustaining local hydrology, supporting agriculture, and also influence the sediment transport within the watershed. Flat or gently sloping terrain typically exhibits a dendritic drainage pattern, which denotes several sub-watersheds with smaller tributaries that feed into more significant streams. The morphology of the watershed is characterized by rugged Siwalik hills, steep slopes, fluvial terraces, which plays important role in sediment transportation and river meandering patterns.

The central to southern portions of the watershed have the highest drainage density (18.1-21 km/km<sup>2</sup>), whereas the watershed boundary with lower-order streams has the lowest drainage density (1- 4.5 km/km<sup>2</sup>) (Figure 3(c)). With elevations ranging from 2020 m in the northwest to 190 m in the southern plain, the geomorphology consists of fertile terraces in the lower regions and depressed landforms in the upper stretches. Diverse landforms are produced by the Bakiya River and its tributaries, with steep slopes in the upper region and noticeable fertile terraces in the lower region (Figure 3(a)). Sal forest covers 78.33% of the watershed area, followed by stream areas (0.3 %), bar deposits (0.65%), settlement (0.77%), cultivable land (8.3%), and barren land 11.5% (Figure 3(d)).

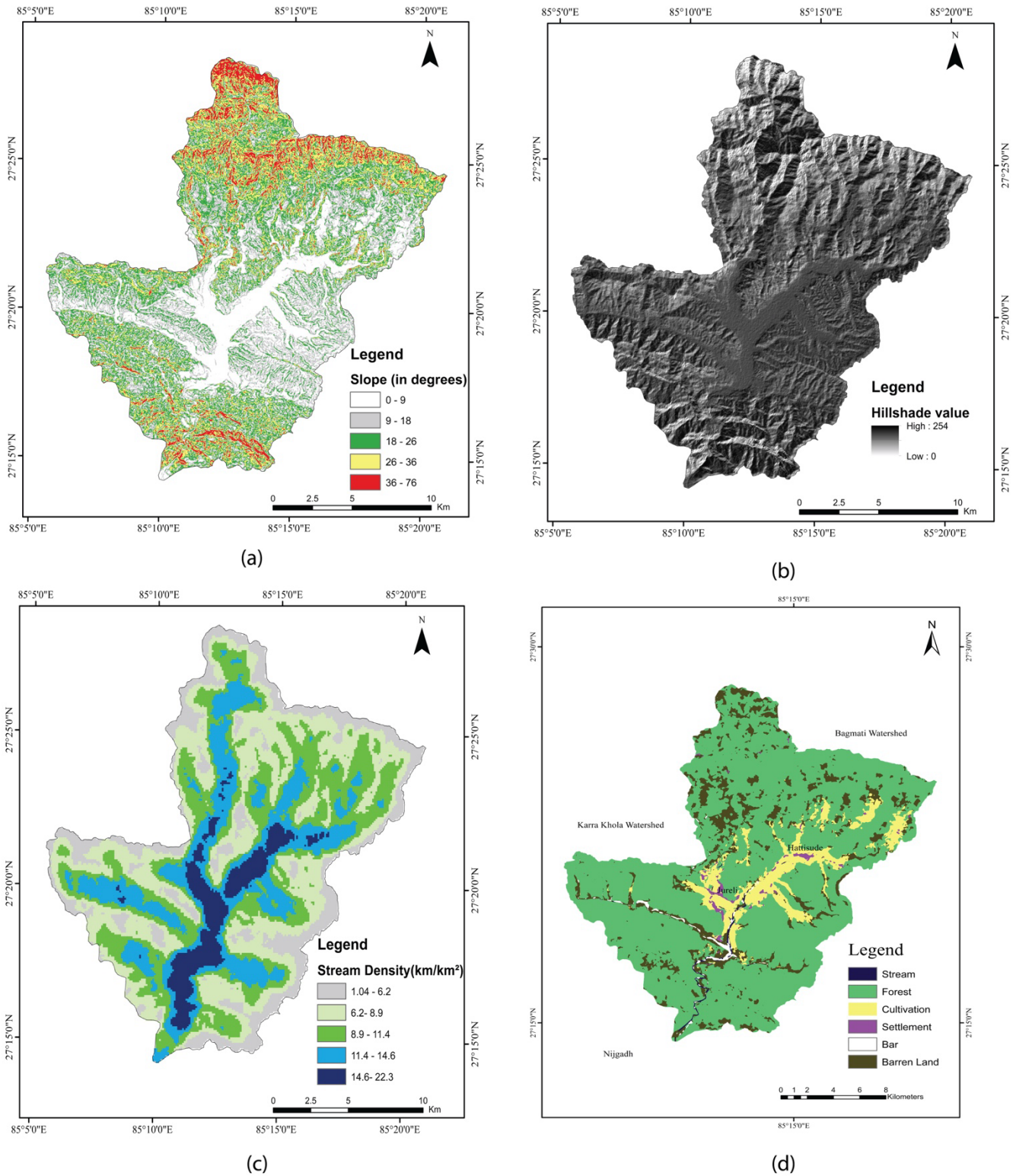


Figure 3 (a) Slope map, (b) Hillshade map, (c) Stream density map, (d) Landuse map of Bakiya watershed

#### 4.2 Morphohydrologic parameters

Rosgen stream classification helps deal with the morphology and hydrologic characteristics of the Bakiya watershed. The various parameters have been measured which are responsible for the river's behavior. For the study of morphohydrologic parameters, the section of the river has been divided into 17 major transects. Figure 4 illustrates

the location of various transects. Similarly, Table 1 provides all the morpho-hydraulic parameters of those cross-sections. The Manning roughness coefficient "n" ranges from 0.035 to 0.515, while 0.06 being the average. The velocity calculated at transects ranges from 0.05 m/s to 2.5 m/s, while 0.764 m/s being the average. The discharge ranges from 0.0513 m<sup>3</sup>/s to 60 m<sup>3</sup>/s, while 8.16 m<sup>3</sup>/s being the average (Table 2).

The Bakiya River's **bankfull width** ranges from 17 meters to 218 meters, averaging 85 meters, with a narrower width near the southeast of Hattisude Bajar, where anthropogenic impacts over the last 20 years have significantly reduced it. The **bankfull area** varies from 18.28 m<sup>2</sup> at T3 to 679.93 m<sup>2</sup> at T17, with an average of 228.3 m<sup>2</sup>, increasing after Hattisude Bajar due to a decrease in slope. The **bankfull depth** spans 0.7 m at T10 to 6.21 m at T17, averaging 2.63 m, while the **thalweg depth** ranges from 0.1 m (T1 and T7) to 0.58 m at T10, with an average of 0.26 meters. The **width-to-depth ratio** is between 15.8 at T3 and 216.2 at T9, averaging 56.7, and the **flood-prone width** ranges from 54 m at T4 to 1438.5 m at T10, with an average of 397.4 m. The **entrenchment ratio** ranges from 1.09 at T16 to 6.19 at T17, with an average of 3.13. The **wetted perimeter** varies from 3.4 m at T1 to 28 m at T16, averaging 15.73 m, and the **cross-sectional area** ranges from 0.436 m<sup>2</sup> at T1 to 24 m<sup>2</sup> at T10, with an average of 5.65 m<sup>2</sup>. The **hydraulic radius** spans 0.134 m at T6 to 1.243 m at T10, averaging 0.366 m, and the **bed slope** varies from 0.0031 m/m at T14 to 0.042 m/m at T1, averaging 0.0096 m/m. The sediment sizes **D50** range from 0.011 m at T1 to 0.05 m at T3, averaging 0.0305 m, and **D84** sizes range from 0.023 m to 0.21 m, with an average of 0.0851 m.

The highest boundary shear stress calculated is 82.92 N/m<sup>2</sup> in transect 10, the lowest is 3.11 N/m<sup>2</sup> in transect 8, and the average is 24.09 N/m<sup>2</sup>. The highest critical shear stress is 37.12 N/m<sup>2</sup> at Transect 3, the lowest is 8.16 N/m<sup>2</sup> at Transect 1, and the average critical shear stress is 21.95 N/m<sup>2</sup>. Similarly, The highest stream power is 4022.4 N/s/m at Transect 10, the lowest stream power is 5.3 N/s/m at Transect 3, and the average stream power across all transects is 374.2 N/s/m.

Table 1: Morphohydraulic parameters estimation at various transects of Bakiya River

| Transects | W <sub>bkf</sub><br>(m) | A <sub>bkf</sub><br>(m <sup>2</sup> ) | D <sub>bkf</sub><br>(m) | Thalweg<br>(m) | W/D<br>ratio | W <sub>fpa</sub> (m) | W <sub>fpa</sub> /W <sub>bkf</sub> | WP<br>(m) | C.S.A.<br>of<br>water<br>(m <sup>2</sup> ) | R <sub>bkf</sub><br>(m) | S <sub>avg</sub><br>(m/m) | D <sub>50</sub><br>(m) | D <sub>84</sub><br>(m) | Sinuosity(K) |
|-----------|-------------------------|---------------------------------------|-------------------------|----------------|--------------|----------------------|------------------------------------|-----------|--|-------------------------|---------------------------|------------------------|------------------------|--------------|
| T1        | 33                      | 38.21                                 | 1.75                    | 0.1            | 28.49        | 86.5                 | 2.62                               | 3.4       | 0.463                                      | 0.136                   | 0.0419                    | 0.011                  | 0.023                  | 1.11         |
| T2        | 34                      | 21.88                                 | 2.05                    | 0.12           | 21.88        | 64.5                 | 1.89                               | 11.63     | 1.67                                       | 0.144                   | 0.028                     | 0.033                  | 0.11                   | 1.2          |
| T3        | 17                      | 18.28                                 | 1.49                    | 0.22           | 15.8         | 70.7                 | 4.16                               | 5.74      | 1.11                                       | 0.193                   | 0.01                      | 0.05                   | 0.21                   | 1.27         |
| T4        | 22                      | 24.78                                 | 1.52                    | 0.18           | 19.52        | 54                   | 2.45                               | 5.91      | 0.89                                       | 0.151                   | 0.017                     | 0.03                   | 0.205                  | 1.31         |
| T5        | 36                      | 53.95                                 | 1.81                    | 0.15           | 24.02        | 184.2                | 5.12                               | 21.26     | 6.34                                       | 0.298                   | 0.0072                    | 0.025                  | 0.07                   | 1.48         |
| T6        | 33                      | 37.29                                 | 1.51                    | 0.21           | 29.2         | 74                   | 2.24                               | 7.59      | 1.02                                       | 0.134                   | 0.0061                    | 0.034                  | 0.061                  | 1.37         |
| T7        | 100                     | 130.1                                 | 1.6                     | 0.1            | 76.87        | 399.5                | 4                                  | 24.9      | 7.18                                       | 0.288                   | 0.0045                    | 0.022                  | 0.048                  | 1.27         |
| T8        | 74                      | 36.43                                 | 0.7                     | 0.18           | 150          | 91.7                 | 1.24                               | 15.4      | 2.32                                       | 0.151                   | 0.0021                    | 0.021                  | 0.037                  | 1.15         |
| T9        | 163                     | 122.85                                | 1.49                    | 0.2            | 216.2        | 438                  | 2.69                               | 11.1      | 3.61                                       | 0.325                   | 0.0026                    | 0.022                  | 0.052                  | 1.35         |
| T10       | 138.5                   | 165.19                                | 2.53                    | 0.58           | 116          | 1438.5               | 10.38                              | 19.3      | 24   | 1.243                   | 0.0068                    | 0.018                  | 0.104                  | 1.18         |
| T11       | 118.5                   | 274.45                                | 2.26                    | 0.29           | 118.77       | 201                  | 1.33                               | 19.62     | 3.21                                       | 0.164                   | 0.0077                    | 0.021                  | 0.055                  | 1.15         |
| T12       | 218.4                   | 499.8                                 | 2.76                    | 0.34           | 95.45        | 1046.15              | 4.79                               | 15        | 10.95                                      | 0.730                   | 0.0053                    | 0.048                  | 0.104                  | 1.52         |
| T13       | 73.5                    | 104.01                                | 2.58                    | 0.37           | 51.94        | 141.5                | 1.92                               | 13.29     | 5.03                                       | 0.379                   | 0.0061                    | 0.045                  | 0.08                   | 1.39         |
| T14       | 70.5                    | 222.61                                | 5.05                    | 0.25           | 14.33        | 111.7                | 1.97                               | 23.55     | 8.43                                       | 0.358                   | 0.0031                    | 0.029                  | 0.06                   | 1.86         |
| T15       | 81                      | 310.47                                | 4.56                    | 0.43           | 21.13        | 205                  | 2.53                               | 10.63     | 2.5  | 0.235                   | 0.0056                    | 0.035                  | 0.08                   | 1.32         |
| T16       | 86.5                    | 314.02                                | 3.98                    | 0.14           | 23.82        | 94.5                 | 1.09                               | 28.16     | 7.36                                       | 0.261                   | 0.0049                    | 0.034                  | 0.085                  | 1.11         |
| T17       | 148                     | 679.93                                | 6.21                    | 0.43           | 32.21        | 917                  | 6.19                               | 23.62     | 15.84                                      | 0.671                   | 0.0057                    | 0.03                   | 0.083                  | 1.08         |

Here, W<sub>bkf</sub> - Bankfull width, A<sub>bkf</sub> - Bankfull area, D<sub>bkf</sub> - Bankfull depth, W/D ratio - Width/depth ratio, W<sub>fpa</sub> - Flood prone width, W<sub>fpa</sub>/W<sub>bkf</sub> - Entrenchment ratio, WP - Wetted perimeter, R<sub>bkf</sub>- hydraulic radius, S<sub>avg</sub>- bed slope

Table 2: Estimation of channel conditions, discharge, and velocity at various transects of Bakiya River

| Transect | n1    | n2    | n3    | n4    | nb    | m   | Manning value 'n' | Slope (s) | Discharge (Q) (m <sup>3</sup> /s) | Velocity(v) (m/s) | D <sub>50</sub> (m) | R <sub>bkf</sub> (m) | Boundary Shear Stress( $\tau_b$ ) (N/m <sup>2</sup> ) | Critical Shear Stress ( $\tau_c$ ) (N/m <sup>2</sup> ) | Stream Power ( $\Omega$ ) (N/s/m) |
|----------|-------|-------|-------|-------|-------|-----|-------------------|-----------|-----------------------------------|-------------------|---------------------|----------------------|---|--|-----------------------------------|
| T1       | 0.002 | 0.003 | 0.001 | 0.003 | 0.03  | 1   | 0.039             | 0.0419    | 0.643                             | 1.389             | 0.011               | 0.136                | 55.90   | 8.16   | 264.3                             |
| T2       | 0.005 | 0.004 | 0.025 | 0.010 | 0.032 | 1.2 | 0.09              | 0.028     | 0.0853                            | 0.05              | 0.033               | 0.144                | 39.55   | 24.5   | 23.4                              |
| T3       | 0.007 | 0.002 | 0.012 | 0.005 | 0.034 | 1.2 | 0.069             | 0.01      | 0.0537                            | 0.048             | 0.05                | 0.193                | 18.93   | 37.12  | 5.3                               |
| T4       | 0.003 | 0.001 | 0.002 | 0.015 | 0.032 | 1.2 | 0.0644            | 0.017     | 0.0513                            | 0.057             | 0.03                | 0.151                | 25.18   | 22.27  | 8.5                               |
| T5       | 0.002 | 0.000 | 0.001 | 0.004 | 0.031 | 1.2 | 0.0437            | 0.0072    | 5.492                             | 0.866             | 0.025               | 0.298                | 21.04   | 18.56  | 387.9                             |
| T6       | 0.001 | 0.001 | 0.002 | 0.002 | 0.032 | 1.2 | 0.0437            | 0.0061    | 0.477                             | 0.467             | 0.034               | 0.134                | 8.018   | 25.24  | 28.5                              |
| T7       | 0.002 | 0.001 | 0.002 | 0.003 | 0.031 | 1.2 | 0.0448            | 0.0045    | 4.709                             | 0.654             | 0.022               | 0.288                | 12.71   | 16.33  | 207.8                             |
| T8       | 0.001 | 0.000 | 0.001 | 0.002 | 0.031 | 1   | 0.035             | 0.0021    | 0.855                             | 0.368             | 0.021               | 0.151                | 3.11  | 15.59  | 17.7                              |
| T9       | 0.001 | 0.002 | 0.001 | 0.002 | 0.031 | 1.2 | 0.0426            | 0.0026    | 2.042                             | 0.565             | 0.022               | 0.325                | 8.29  | 16.33  | 52.1                              |
| T10      | 0.001 | 0.003 | 0.001 | 0.002 | 0.031 | 1   | 0.038             | 0.0068    | 60.298                            | 2.512             | 0.018               | 1.243                | 82.92   | 13.36  | 4022.4                            |
| T11      | 0.001 | 0.001 | 0.004 | 0.01  | 0.031 | 1   | 0.047             | 0.0077    | 1.796                             | 0.559             | 0.021               | 0.164                | 12.38   | 15.59  | 135.7                             |
| T12      | 0.006 | 0.004 | 0.002 | 0.002 | 0.034 | 1.3 | 0.0624            | 0.0053    | 10.33                             | 0.943             | 0.048               | 0.73                 | 37.95   | 35.64  | 537.1                             |
| T13      | 0.006 | 0.000 | 0.004 | 0.002 | 0.031 | 1.2 | 0.0495            | 0.0061    | 4.164                             | 0.827             | 0.045               | 0.379                | 22.67   | 33.41  | 249.2                             |
| T14      | 0.002 | 0.001 | 0.002 | 0.002 | 0.032 | 1.3 | 0.515             | 0.0031    | 4.588                             | 0.544             | 0.029               | 0.358                | 10.88   | 21.53  | 139.6                             |
| T15      | 0.001 | 0.002 | 0.002 | 0.002 | 0.032 | 1.2 | 0.045             | 0.0056    | 1.593                             | 0.637             | 0.035               | 0.235                | 12.91   | 25.98  | 87.6                              |
| T16      | 0.002 | 0.003 | 0.01  | 0.002 | 0.031 | 1   | 0.048             | 0.0049    | 4.442                             | 0.604             | 0.034               | 0.261                | 12.55   | 25.24  | 213.5                             |
| T17      | 0.003 | 0.000 | 0.006 | 0.002 | 0.032 | 1   | 0.053             | 0.0057    | 17.294                            | 0.46              | 0.03                | 0.671                | 37.52   | 22.27  | 967.1                             |

Here, n1= Degree of irregularity, n2= Variation in channel cross-section, n3= effect of obstructions, n4= amount of vegetation, nb= base value of manning for straight river, m= sinuosity, n= manning coefficient.

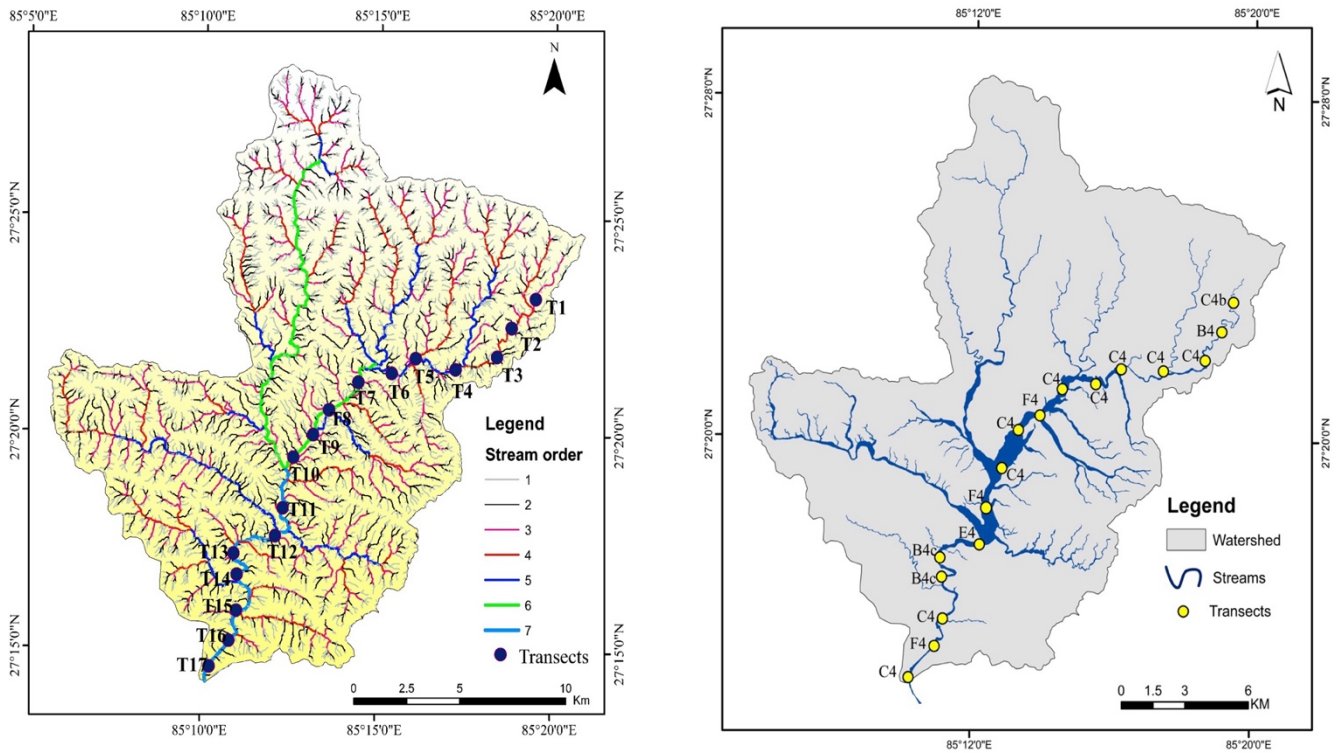


Figure 4: Stream order map with location of transects (left) and Rosgen-classified streams Level II (right)

### 4.3 Classification of stream (Rosgen Level I and Level II)

The stream classification was conducted on 17 transects starting from the lower order streams. They are classified as T1-C4b, T2-B4, T3-C4, T4-C4, T5-C4, T6-C4, T7-C4, T8-F4, T9-C4, T10-C4, T11-F4, T12-E4, T13-B4c, T14-B4c, T15-C4, T16-F4 and T17- C4 (Table 4). Most of the transects belong to the C4 category, followed by B4, F4, and E4.

Table 3: Rosgen LEVEL I classification at various transects

| Transect | Stream order | Valley Type | W/D Ratio | Sinuosity | Slope (m/m) | Stream Type |
|----------|--------------|-------------|-----------|-----------|-------------|-------------|
| 1        | 4            | VIII        | >12       | 1.11      | 0.0419      | C           |
| 2        | 4            | II          | >12       | 1.2       | 0.028       | B           |
| 3        | 4            | VIII        | >12       | 1.27      | 0.01        | C           |
| 4        | 5            | VIII        | >12       | 1.31      | 0.017       | C           |
| 5        | 5            | VIII        | >12       | 1.48      | 0.0072      | C           |
| 6        | 5            | VIII        | >40       | 1.37      | 0.0061      | C           |
| 7        | 6            | VIII        | >40       | 1.27      | 0.0045      | C           |
| 8        | 6            | VIII        | >40       | 1.15      | 0.0021      | F           |
| 9        | 6            | VIII        | >40       | 1.35      | 0.0026      | C           |
| 10       | 6            | VIII        | >40       | 1.18      | 0.0068      | C           |
| 11       | 7            | VIII        | >40       | 1.15      | 0.0077      | F           |
| 12       | 7            | VIII        | >40       | 1.52      | 0.0053      | E           |
| 13       | 7            | VI          | >40       | 1.39      | 0.0061      | B           |
| 14       | 7            | VI          | >12       | 1.86      | 0.0031      | B           |
| 15       | 7            | VI          | >12       | 1.32      | 0.0056      | C           |
| 16       | 7            | VI          | >12       | 1.11      | 0.0049      | F           |
| 17       | 7            | VIII        | >12       | 1.08      | 0.0057      | C           |

Table 4: Rosgen LEVEL II classification at various transects

| Transect | Stream order | Entrenchment Ratio | W/D Ratio | Sinuosity | Slope (m/m) | D <sub>50</sub> (m) | Stream Type |
|----------|--------------|--------------------|-----------|-----------|-------------|---------------------|-------------|
| 1        | 4            | >2.2               | >12       | 1.11      | 0.0419      | 0.011               | C4b         |
| 2        | 4            | 1.4-2.2            | >12       | 1.2       | 0.028       | 0.033               | B4          |
| 3        | 4            | >2.2               | >12       | 1.27      | 0.01        | 0.05                | C4          |
| 4        | 5            | >2.2               | >12       | 1.31      | 0.017       | 0.03                | C4          |
| 5        | 5            | >2.2               | >12       | 1.48      | 0.0072      | 0.025               | C4          |
| 6        | 5            | >2.2               | >40       | 1.37      | 0.0061      | 0.034               | C4          |
| 7        | 6            | >2.2               | >40       | 1.27      | 0.0045      | 0.022               | C4          |
| 8        | 6            | <1.4               | >40       | 1.15      | 0.0021      | 0.021               | F4          |
| 9        | 6            | >2.2               | >40       | 1.35      | 0.0026      | 0.022               | C4          |
| 10       | 6            | >2.2               | >40       | 1.18      | 0.0068      | 0.018               | C4          |
| 11       | 7            | <1.4               | >40       | 1.15      | 0.0077      | 0.021               | F4          |
| 12       | 7            | >2.2               | >40       | 1.52      | 0.0053      | 0.048               | E4          |
| 13       | 7            | 1.4-2.2            | >40       | 1.39      | 0.0061      | 0.045               | B4c         |
| 14       | 7            | 1.4-2.2            | >12       | 1.86      | 0.0031      | 0.029               | B4c         |
| 15       | 7            | >2.2               | >12       | 1.32      | 0.0056      | 0.035               | C4          |
| 16       | 7            | <1.4               | >12       | 1.11      | 0.0049      | 0.034               | F4          |
| 17       | 7            | >2.2               | >12       | 1.08      | 0.0057      | 0.03                | C4          |

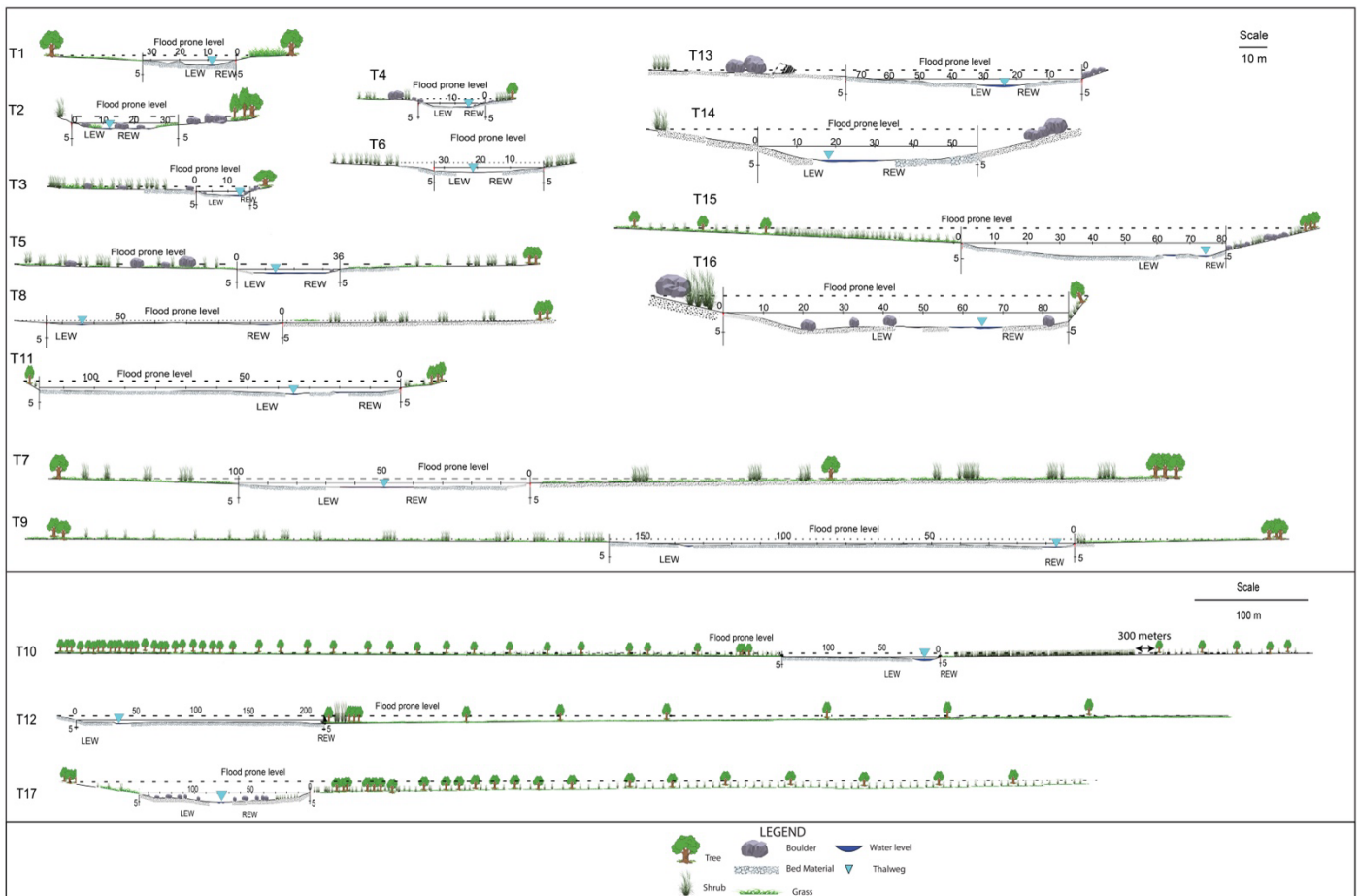


Figure 5: Cross-section of Bakiya River from T1 to T17

The C4 streams are slightly entrenched, meandering, gravel-dominated with the well-developed floodplain. They have broad river valleys with coarse alluvium and have slopes under 2%. Similarly, the stream banks are composed of unconsolidated, heterogeneous, non-cohesive, alluvial materials that are finer than the gravel-dominated bed material (Figure 6). These streams are also susceptible to accelerated bank erosion, and the rate of lateral adjustment is directly influenced by the presence of vegetation. They have many point bars, but the sediment supply is moderate to high (Rosgen, 1994).

The B4 streams are moderately entrenched with landforms gentle to rolling slopes in relatively narrow, colluvial valleys. They have predominantly gravel, followed by boulders, gravel, and sand. They have irregular spaces scour pools (Figure 6). There are relatively stable and not high sediment supply stream channels (Rosgen, 1994).

The F4 streams are gravel-dominated, entrenched, meandering channels deeply incised and have gentle terrain. The slopes are generally under 2%. The dominant channel materials are gravel, followed by cobble and sand (Figure 6). The sediment supply is moderate to high. The flood plain is often developed inside the bankfull channel (Rosgen, 1994). The E4 streams are channel systems with low to moderate sinuosity, gentle to moderately steep channel gradients, with low channel width to depth ratio. They are found in broad alluvial valleys with well-developed floodplain (Rosgen, 1994) (Figure 6).

In a nutshell, the streams are C4, B4, F4, and E4, each with distinct characteristics. C4 streams are meandering, gravel-dominated, with well-developed floodplains and slopes under 2%, while B4 streams are moderately entrenched with gravel and boulders, exhibiting more stable channels and a lower sediment supply.



Figure 6: The third transect-C4 stream (upper left), second transect-B4 stream (upper right), sixteenth transect-F4 stream (lower left), and twelfth transect-E4 stream (lower right)

The discharge and velocity measurements for the 17 transects demonstrated significant variation across the study area. The river discharge ranged from a minimum of 0.0513 cubic meters per second ( $\text{m}^3/\text{s}$ ) at Transect 4 to a maximum of 60.298  $\text{m}^3/\text{s}$  at Transect 10. Notably, high discharge values were also observed at Transect 12 (10.33  $\text{m}^3/\text{s}$ ) and Transect 17 (17.294  $\text{m}^3/\text{s}$ ). The velocity variations followed a similar trend, with velocities ranging from 0.048 meters per second ( $\text{m}/\text{s}$ ) at Transect 3 to 2.512  $\text{m}/\text{s}$  at Transect 10. Other significant velocities were recorded at Transect 12 (0.943  $\text{m}/\text{s}$ ) and Transect 7 (0.654  $\text{m}/\text{s}$ ).

Overall, the data indicate that certain transects, such as transect 10 and transect 12, exhibit markedly higher discharge and velocity values, suggesting areas of greater flow and potential energy within the river system. Conversely, transects with lower discharge and velocity measurements, such as Transect 3 and Transect 4, indicate slower and steadier flow conditions.

## 5. Discussions

The Bakiya watershed is a dynamic geomorphological system as it is located in the tectonically active Siwalik range of Nepal Himalaya. The factors such as lithological weaknesses, intense monsoon rainfall, and anthropogenic impacts make it prone to erosion, flooding, landslides, etc. (Bhandari & Dhakal, 2019, 2020). The central and southern region has high stream density as compared to the northern and boundary regions indicating the potential erosion and intense surface runoff. The uppermost region is characterized by a steep slope transitioning to fertile terraces in the lower stretches. These terraces are the depositional zones and are influenced by sediment transport and reduced slope gradients. Transect 10 has the highest boundary shear stress ( $82.92 \text{ N}/\text{m}^2$ ) and stream power ( $4022.4 \text{ N}/\text{s}/\text{m}$ ), which displays high-energy flows that aid in erosion and sediment transport. In contrast,

other transects have lower shear stress and stream power, which are associated with flatter slopes and depositional zones.

Bakiya River's morpho-hydraulic parameters display notable variations downstream that are similar to those observed in other river systems, including the Godavari Khola (Karki et al., 2016) and the Karra Khola (Subedi & Tamrakar, 2020). The bankfull width of the Bakiya River ranges from 17 m to 218 m (average: 85 m), and the bankfull area varies between 18.28 m<sup>2</sup> and 679.93 m<sup>2</sup> (average: 228.3 m<sup>2</sup>). This variability is characteristic of mid-order streams with moderate to low entrenchment. Similar trends were noted in the Karra Khola, where geomorphic processes are reflected in dynamic changes in bankfull dimensions and meander belt widths (Subedi & Tamrakar, 2020). Similar downstream widening in the Doodhganga stream has been ascribed to geomorphic influences and water extraction according to (Hussain & Pandit 2011). Similar variability has been observed in streams that are slightly to moderately entrenched in the Chequamegon National Forest (CNNF), which is consistent with these trends (Savery et al., 2001). The velocity in the Bakiya River fluctuates between 0.048 m/s and 2.512 m/s, while the discharge ranges from 0.0513 m<sup>3</sup>/s to 60.298 m<sup>3</sup>/s. These figures demonstrate the downstream effects of tributary contributions and a decline in channel roughness. Thalweg depths in the Bakiya River range from 0.1 m to 0.58 m (average: 0.26 m), with a downstream increase that corresponds to greater sediment transport and flow energy. Width-to-depth ratios (15.8–216.2, average: 56.7) reflect progressive channel widening. Similar patterns were observed in the Godavari Khola and Karra Khola (Karki et al., 2016; Subedi & Tamrakar, 2020). In these systems, tributary inputs increase sediment loads and discharge downstream, emphasizing the dynamic interplay between channel morphology and hydraulics.

Similar widening is consistent with findings in CNNF (Savery et al., 2001) and the Doodhganga stream (Hussain & Pandit, 2011), where channel materials and entrenchment levels influence downstream morphology. The Bakiya River's flood-prone widths (54–1,438.5 m, average: 397.4 m) and entrenchment ratios (1.09–6.19, average: 3.13) classify it as slightly to moderately entrenched, similar to C4-dominated stream types in the Karra and Godavari Khola (Karki et al., 2016; Subedi & Tamrakar, 2020). The highest boundary shear stress calculated is 82.92 N/m<sup>2</sup> in transect 10, the lowest is 3.11 N/m<sup>2</sup> in transect 8, and the average is 24.09 N/m<sup>2</sup>. This represents the direct relationship with hydraulic radius and slope. The average critical shear stress is 21.95 N/m<sup>2</sup>, while the highest is 37.12 N/m<sup>2</sup> at Transect 3, and the lowest is 8.16 N/m<sup>2</sup> at Transect 1, which corresponds to the lowest median sized sediments at transect 1 and highest at transect 3. Similarly, transect 10 has the highest stream power at 4022.4 N/s/m. Transect 3 has the lowest at 5.3 N/s/m, and the average for all transects is 374.2 N/s/m, which displays the highest discharge and slope at transect 10 and lowest at transect 3.

The stream power observed at various transects (5.3 to 4022 N/s) display huge fluctuation along the stream of transporting capacity. This may be probably due to change in slope and stream pattern (Kazi Tamrakar et al., 2011). The hydraulic parameters of the Bakiya River, including Manning's roughness coefficient (0.035–0.515, average: 0.06) and hydraulic radius (0.134–1.243 m, average: 0.366 m), are consistent with gently sloping meandering streams. Its slope (0.0031–0.042 m/m, average: 0.0096 m/m) displays the low-gradient streams. These patterns align with what has been observed in CNNF (Savery et al., 2001) and Doodhganga (Hussain & Pandit, 2011), where the slopes change from steeper upstream sections to softer downstream gradients depending on the relief of the terrain. The Bakiya River sediment distribution varies from coarse boulders and sandy gravel upstream to finer gravelly sand and muddy sand downstream. (Karki et al., 2016) describe the Godavari Khola shows a similar fining downward sequence indicating a reduction in transport energy, and similar trends can be observed in CNNF and Doodhganga downstream (Hussain & Pandit, 2011; Savery et al., 2001).

Stream types found in the Bakiya River are primarily C4, which are defined by low-sloped gravel-dominated meandering and somewhat entrenched channels. In Karra Khola, most of the segment of the main stream flowing through the broad multi-river terraces and broad flood plain are entrenched and fall under the C-type of the stream (Subedi & Tamrakar 2020). 19 out of 121 reaches were categorized as C4 type streams in CNNF, which is the most after the E5 stream type (Savery et al., 2001). Differences in sediment gradation and width-to-depth ratios highlight

localized geomorphic and anthropogenic factors that affect stream morphology. A similar dominance of C4 stream types with gentle entrenchment and gravel-dominated meandering channels was noted by (Phillips & Desloges, 2015). The C4 streams are meandering, gravel-dominated, with well-developed floodplains and slopes under 2%, while B4 streams are moderately entrenched with gravel and boulders, exhibiting more stable channels and a lower sediment supply. Rosgen Classification System can be used to distinguish between stable and unstable stream reaches based on pivotal morphological parameters. RCS also stresses the importance of extending research into vegetation dynamics and management effects, as well as evaluating the system's applicability across various riparian ecosystems for broader ecological and management implications (Meehan & O'Brien, 2019).

## 6. Conclusions

Depending on how each transect is classified, the analysis of stream types across transects (T1 to T17) reveals unique spatial distribution stability and management requirements. Present in 10 out of the 17 transects (T1, T3, T4, T5, T6, T7, T9, T10, T15, and T17), the predominance of C streams (C4b and C4) highlights the existence of wide low-gradient valleys with floodplain connectivity and reasonably stable meandering channels. These streams mainly depend on vegetation for stability with medium energy and a high sediment load. Strong vegetation stabilization and reduction of disturbances should be the top priorities for effective management of these transects as they might worsen sediment transport and erosion (Rosgen, 2001). Three transects (T2, T13, and T14) contain B streams (B4, B4c) which indicate areas with moderate stability and narrow, gently sloping valleys. Because of their high energy and step-pool morphology, these streams need to have their vegetation and sediment load closely monitored in order to preserve their moderate stability (Rosgen, 2001). Wide valley meadows are stable and effective low-energy systems known as E streams (E4), which were identified in T12. T12, a stream that heavily depends on vegetation for stability, has a high potential for restoration and is a priority for conservation. Its meandering morphology should be preserved, and strong vegetative support should be guaranteed (Rosgen, 2001). Regions with significant entrenchment and lateral instability are highlighted by F streams (F4), which are found in T8, T11, and T16. These streams have mixed energy dynamics, high width-to-depth ratios, and a high degree of erosion susceptibility. These transects require engineered interventions like bank stabilization and sediment load management to reduce the risks of erosion and instability (Rosgen, 2001).

As a result of the region's low gradient and alluvial systems sensitivity to human alteration, the overall distribution highlights the predominance of C streams. While F streams indicate zones most affected by geomorphic instability and in need of urgent attention, the presence of B streams indicates areas of moderate relief with transitional stability. A crucial area for conservation efforts is the isolated E stream at T12, which is notable for its efficiency and stability.

**Acknowledgment:** The authors are thankful to the Central Department of Geology, Tribhuvan University for providing the necessary survey equipments.

## References

- [1] Aldridge, B. N., & Garrett, J. M. (1973). Roughness coefficients for stream channels in Arizona. In *Open-File Report* (Issue February).
- [2] Arcement, G. J., & Schneider, V. R. (1989). Guide for selecting Manning's roughness coefficients for natural channels and flood plains. *US Geological Survey Water-Supply Paper*, 2339.
- [3] Bhandari, B. P., & Dhakal, S. (2018). Lithological Control on Landslide in the Babai Khola Watershed, Siwaliks Zone of Nepal. *American Journal of Earth Sciences*, 5(3).
- [4] Bhandari, B. P., & Dhakal, S. (2019). Evolutional Characteristics of Debris Flow in the Siwalik Hills of Nepal. *International Journal of Geosciences*, 10(12). <https://doi.org/10.4236/ijg.2019.1012060>
- [5] Bhandari, B. P., & Dhakal, S. (2020). Spatio-temporal dynamics of landslides in the sedimentary terrain: a case of Siwalik zone of Babai watershed, Nepal. *SN Applied Sciences*, 2(5). <https://doi.org/10.1007/s42452-020-2628-0>
- [6] Castro, J. M., & Jackson, P. L. (2001). Bankfull discharge recurrence intervals and regional hydraulic geometry relationships: Patterns in the Pacific Northwest, USA. *Journal of the American Water Resources Association*, 37(5). <https://doi.org/10.1111/j.1752-1688.2001.tb03636.x>

- [7] Chow, V. Te. (1959). *Open-Channel Hydraulics*. Ven Te Chow. McGraw-Hill, New York, 1959. xviii+ 680 pp. Illus. \$17. *Science*, 131(3408).
- [8] Cowan, W. L. (1956). Estimating Hydraulic Roughness Coefficients. *Agricultural Engineering ASAE*.
- [9] Department of Mines and Geology. (2002). *Geological map of Petroleum Exploration Block-7, Malangawa, Central Nepal (DMG/HMGN)*.
- [10] Hussain, Q., & Pandit, A. (2011). Hydrology, geomorphology, and Rosgen classification of Doodhganga stream in Kashmir Himalaya, India. *International Journal of Water Resources and Environmental Engineering*, 3(3).
- [11] Jefferson N. Keaton, T. M. and E. J. D. (2005). Development and analysis of regional curves for streams in the non-urban valley and ridge physiographic province, Maryland, Virginia, and West Virginia. *Scientific Investigations Report*.
- [12] Karki, S. S., Kazi Tamrakar, N., Khola, D., & Khola, L. (2016). *Fluvial morphology and dynamics of the Godavari Khola, southeast Kathmandu, Central Nepal* (Vol. 19).
- [13] Kazi Tamrakar, N., Bajracharya, R., & Shrestha, P. (2011). *River dynamics and existing stability condition of the Manahara River, Kathmandu basin, Central Nepal Himalaya* (Vol. 14).
- [14] Kizaki, K. (1994). An outline of Himalayan upheaval. *Jagadamba Prakashan, Kathmandu*.
- [15] Leopold, L. B., & Wolman, M. G. (1957). River channel patterns: braided, meandering, and straight. *USGS Professional Paper*, 282-B.
- [16] Meehan, M. A., & O'Brien, P. L. (2019). Using the Rosgen Stream Classification System to Aid in Riparian Complex Ecological Site Descriptions Development. *Rangeland Ecology and Management*, 72(5), 729–735. <https://doi.org/10.1016/j.rama.2019.05.001>
- [17] Montgomery, D. R., & B. J. M. (1993). A field survey of channel processes for several gravel-bed rivers. *Water Resources Research*.
- [18] Phillips, R. T. J., & Desloges, J. R. (2015). Glacial legacy effects on river landforms of the southern Laurentian Great Lakes. *Journal of Great Lakes Research*, 41(4), 951–964. <https://doi.org/10.1016/j.jglr.2015.09.005>
- [19] Rosgen, D. L. (1994). A classification of natural rivers. *Catena*, 22(3). [https://doi.org/10.1016/0341-8162\(94\)90001-9](https://doi.org/10.1016/0341-8162(94)90001-9)
- [20] Rosgen, D. L. (2001). A stream channel stability assessment methodology. *Proceedings of the Seventh Federal Interagency Sedimentation Conference, March 25-29, 2001, Reno, Nevada (USA)*, 1.
- [21] Rust, B. R. (1977). A classification of alluvial channel systems. *Canadian Society of Petroleum Geology Memoir*, 5, 187-198.
- [22] Savery, T. S., Belt, G. H., & Higgins, D. A. (2001). Evaluation of the Rosgen Stream Classification System in Chequamegon-Nicolet National Forest, Wisconsin. *Journal of the American Water Resources Association*, 37(3). <https://doi.org/10.1111/j.1752-1688.2001.tb05500.x>
- [23] Schumm, S. A. (1977). *The Fluvial System*. John Wiley and Sons, New York, 338p.
- [24] Shields, I. A. (1936). Application of similarity principles and turbulence research to bed-load movement, U.S. Soil Conservation Service Coop. Lab. In Ott, W.P., van Uchelen, J.C. (Eds.), (Translators), *Hydrodynamics Laboratory Publication*, vol. 167. *California Institute of Technology, Pasadena*.
- [25] Subedi, M., & Tamrakar, N. K. (2020). Fluvial Geomorphology and Basin Development of Karra Khola Basin, Hetauda, Central Nepal. *Journal of Geological Research*, 2(4). <https://doi.org/10.30564/jgr.v2i4.2250>
- [26] Tokuoka, T., Takeda, S., Yoshida, M., & Upreti, B. N. (1988). The Churia (Siwalik) Group in the western part of the Arung Khola area, west central Nepal. *Memoirs of Faculty of Science, Shimane University*, 22, 131-140.
- [27] Tokuoka, T. (1992). The Churai (Siwalik) Group in West Central Nepal. *Bulletin of the Department of Geology, Tribhuvan University*, 22, 75–88.